

## Circularly Polarized Lens Antenna for Tbps Wireless Communications

Campo, Marta Arias; Blanco, Darwin; Carluccio, Giorgio; Litschke, Oliver; Bruni, Simona; Llombart, Nuria

**DOI**

[10.23919/EuMC.2018.8541685](https://doi.org/10.23919/EuMC.2018.8541685)

**Publication date**

2018

**Document Version**

Accepted author manuscript

**Published in**

2018 48th European Microwave Conference (EuMC)

**Citation (APA)**

Campo, M. A., Blanco, D., Carluccio, G., Litschke, O., Bruni, S., & Llombart, N. (2018). Circularly Polarized Lens Antenna for Tbps Wireless Communications. In *2018 48th European Microwave Conference (EuMC)* (pp. 1147-1150). Article 8541685 IEEE. <https://doi.org/10.23919/EuMC.2018.8541685>

**Important note**

To cite this publication, please use the final published version (if applicable). Please check the document version above.

**Copyright**

Other than for strictly personal use, it is not permitted to download, forward or distribute the text or part of it, without the consent of the author(s) and/or copyright holder(s), unless the work is under an open content license such as Creative Commons.

**Takedown policy**

Please contact us and provide details if you believe this document breaches copyrights. We will remove access to the work immediately and investigate your claim.

# Circularly Polarized Lens Antenna for Tbps Wireless Communications

Marta Arias Campo<sup>#\*1</sup>, Darwin Blanco<sup>#2</sup>, Giorgio Carluccio<sup>#3</sup>, Oliver Litschke<sup>\*4</sup>, Simona Bruni<sup>\*5</sup>, Nuria Llombart<sup>#6</sup>

<sup>#</sup> THz Sensing Group, Delft University of Technology, The Netherlands

<sup>\*</sup> IMST GmbH, Kamp-Lintfort, Germany

{<sup>1</sup>M.AriasCampo, <sup>2</sup>D.J.BlancoMontero, <sup>3</sup>G.Carluccio, <sup>6</sup>N.LlombartJuan}@tudelft.nl, {<sup>4</sup>litschke, <sup>5</sup>bruni}@imst.de

**Abstract** — The exponentially increasing demand for high-speed wireless links can be only efficiently satisfied with the development of future XG wireless communication networks, based on higher carrier signal frequencies, starting from 100 GHz. In this contribution, a circularly polarized G-band leaky-wave fed lens antenna with an integrated dielectric grid polarizer is presented, which can fulfill the challenging requirements for these future XG networks. A design is proposed in low dielectric permittivity material with a feed matching better than -10dB over a 44% of relative bandwidth. The circularly polarized lens aperture efficiency is higher than 75% over a 35% relative bandwidth, with an axial ratio lower than 3dB. Analytical tools have been applied to optimize the lens aperture efficiency, validating the results via full wave simulations. A lens prototype has been now fabricated and is currently being measured.

**Keywords** — polarizer, leaky-wave, lens antenna, wideband communications.

## I. INTRODUCTION AND SCENARIO

The increasing demand in the number of simultaneous high-speed wireless connections, as well as the expectations in the quality of these links, in order to support new applications such as virtual reality, 3D photos and videos, and high definition, is leading already to a revolution in the conception of wireless communications systems. Signal processing techniques, which are until now the only strategy to increase the system data rates, are reaching a saturation point which makes it necessary to explore new alternatives in order to further improve wireless system performances. By moving the RF system frequency to higher bands, the link can profit from a larger available RF bandwidth, and so increase the maximum achieved through-put. In [1] an innovative, power-efficient base station architecture for a football stadium scenario, based on a compact system at D-band was proposed. The system is capable of providing 80.000 spectators with 12 Tbps of total capacity, which could be translated in a data rate of 150 Mbps per user. The base station consists of a single, central 3D elliptical lens antenna array containing 1500 transceivers. These establish fixed communication links with each of the 1500 cells in which the stadium is divided, on a SDMA/FDMA scheme. Each transceiver supports a semi-duplex 8Gbps-link, covering a cell of around 50 users. Inside every cell, the users are assigned a certain time slot (TDD), bringing this multiplexing scheme to a high system adaptability in case of variable number of users per cell. In order to achieve the claimed capacity, antennas with 34 dB of

gain with at least 24 GHz of bandwidth have been considered. The use of lens antennas allows us to reach these high antenna directivities avoiding the losses in feeding networks, which would be extremely high in these high frequency bands. Indeed, the optimization of the aperture efficiency for these lenses is crucial, as every dB lost in spillover, reflection, ohmic loss or taper efficiency has a direct impact in the base station achieved data-rate and/or its efficiency in terms of power consumption.

Broadband high aperture efficiency can only be reached in elliptical lenses by avoiding total reflection areas along the entire frequency band. The feeding antenna should therefore illuminate the lens with very symmetric patterns and optimum taper at the edge of the lens. In most of the reported works, the lenses are fed efficiently over a narrow band, using double slot antennas [2] or patches [3]. Although other works present well matched and stable phase center over a very wide band, the reported aperture efficiency is low [4]. In [5] a matching technique is presented for an integrated open waveguide primary source. It achieves 30% relative bandwidth using a small air pocket etched off the dielectric. The reported side-lobe level is however almost -10dB as a consequence of the poor illumination of the lens. In [6] a Leaky-Wave Antenna (LWA) based on a resonant air gap was proposed as a promising solution to act as lens feeders, because of its high directivity, symmetric pattern, compactness, low profile and compatibility with silicon fabrication processes. As the proposed resonant LWA is radiating into a dense dielectric medium, the achieved relative bandwidth is enhanced w.r.t. standard leaky wave or Fabry Perot antennas. Low dielectric permittivity ( $\epsilon_r$ ) materials represent a good candidate to fabricate lens antenna arrays, due to their low loss, light weight and cost-effective manufacturing through processes such as injection molding or 3D printing. The large bandwidth achieved when illuminating the lenses with a LWA feed turns them into a good compromise for our scenario, in terms of RF performance.

In the pursuit of the highest wireless link efficiency, the use of circularly polarized antennas on both the terminal and base station is an additional improvement, as the loss due to polarization misalignment is significantly reduced. Many polarizer concepts have been presented in the low GHz (up to 30 GHz), based mainly on PCB multi-layer designs, such as [7] and [8]. These reach bandwidths up to 35%, keeping a high efficiency. However, the use of very thin metal printed

structures makes them impossible to fabricate in standard PCB technology for frequency bands higher than 100 GHz. In terahertz bands, metal grating polarizers have been introduced in [9], based on the reflection of orthogonal polarizations with  $90^\circ$  of phase shift. They present a narrow bandwidth and cannot be integrated into a lens antenna, resulting in a bulky solution, especially if multi-beams are needed. In optic frequency ranges, dielectric grating polarizers are fabricated in materials such as Ge [10] or Si [11], by means of lithographic etching processes. Those are based on the transmission of orthogonal polarizations with  $90^\circ$  of phase shift. Their efficiency and bandwidth are compromised due to the high reflections in the air-polarizer interface caused by their high  $\epsilon_r$ . Nevertheless, this approach represents the best starting point for our requirements, which can be met again by lowering the material  $\epsilon_r$ . Basing on this concept an optimized polarizer has been designed to be integrated inside the plastic lens (Fig. 1c and Fig. 6a).

This document focuses on the analysis and design of low-density elliptical lenses with integrated circular polarizers, illuminated by resonant LWAs, for broadband wireless communication applications. The goal is to maximize the aperture efficiency over a large frequency band, minimizing as well the axial ratio (AR).

## II. LENS FED BY RESONANT LEAKY-WAVE ANTENNA

In this section, the LWA feeder concept and its performance radiating in an infinite dielectric medium are presented. The results for a lens illuminated by the LWA are shown as well, being both optimized with the goal of maximizing the aperture efficiency over the whole frequency band.

### A. Resonant LWA concept

The physical phenomenon exploited in resonant LWA is the excitation of a pair of nearly degenerated  $TM_1/TE_1$  leaky-wave modes [12]. These modes propagate in a resonant cavity by means of sub-critical multiple reflections between the ground plane and the dielectric (Fig. 1a), increasing the antenna effective area and thus its directivity. This type of LWA generates also an undesired spurious  $TM_0$  leaky-wave mode, conceptually associated with the  $TEM$  mode of the perfectly conducting walls parallel plate waveguide. This undesired mode does not radiate in broadside direction, and therefore can degrade the beam shape. The effect of the  $TM_0$  can be reduced by using a double slot opening in a ground plane (Fig. 1b) as proposed in [13-14]. Moreover the double slot parameters also strongly affect the symmetry of the patterns, and as a consequence the aperture efficiency. Thus including the analytical model of the double slot in the overall analysis allows us to optimize the antenna performance over a broad band. The primary fields (inside the dielectric) are evaluated by using an asymptotic evaluation of the SGF [15] with an infinite dielectric super-layer and the Fourier transform of the currents on the double slot iris, as described in [16].

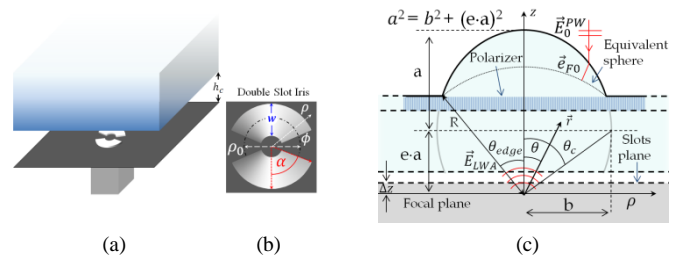


Fig. 1. (a) Geometry of the leaky-wave antenna radiating in a semi-infinite dielectric-slab. The dielectric is located at a distance of  $\lambda_0/2$  to create a Fabry-Perot cavity. (b) Main parameters of the double slot iris and current distribution excited by the  $TE_{01}$  mode of the square waveguide. (c) Elliptical lens geometric parameters, with integrated polarizer.

### B. Feed and lens optimization

The eccentricity of a dielectric elliptical lens is defined exclusively by its material  $\sqrt{\epsilon_r}$ , as  $e = 1/\sqrt{\epsilon_r}$ . Such lenses are characterized by an intrinsic critical angle  $\theta_c$  after which the energy coming from the ellipse focus suffers from total reflection. In order to achieve high reflection efficiency, only the lens region above  $\theta_c$  should be illuminated (top half of the ellipse).  $\theta_c$  depends exclusively on the dielectric  $\epsilon_r$ , and increases for higher values of  $\epsilon_r$  as  $\theta_c = \tan^{-1} \sqrt{\epsilon_r - 1}$ . Thus lenses with lower  $\epsilon_r$  need to be illuminated with more directive beams than denser lenses. In order to maximize the aperture efficiency,  $\eta_{ap}$ , the lens should be truncated at an angle  $\theta_{edge} < \theta_c$  (Fig. 1c).

The feed geometry is optimized in terms of coupling to the lens and impedance matching to a waveguide, in order to achieve the optimum lens  $\eta_{ap}$ . The slots position in  $z$ -direction with respect to the lens focus,  $\Delta z$ , and the ellipse truncation angle,  $\theta_{edge}$ , represent the parameters in this optimization (Fig. 1c).  $\eta_{ap}$  is calculated by evaluating the lens antenna in reception as described in [17]. The power received by the antenna can be related to the field correlation between the primary field and the field incident on the lens, over a sphere surrounding the feed (see Fig. 1c). The field incident on the lens  $\vec{E}_{FO}(\theta, \phi)$  can be evaluated analytically as derived in [18]. This technique allows us to obtain the lens  $\eta_{ap}$  for a known primary pattern,  $\Delta z$  and  $\theta_{edge}$ , with no need to perform the secondary pattern computation, which is more time-consuming. The procedure is described in more detail in [16]. This efficiency  $\eta_{ap}^{FO}$  includes the taper efficiency  $\eta_{tap}$ , the spillover efficiency  $\eta_{so}$  and the reflection efficiency  $\eta_{ref}$ . The only parameter which is not covered is the impedance matching of the antenna, which is evaluated via full-wave electromagnetic commercial software. With this procedure, the parameters  $\Delta z$  and  $\theta_{edge}$  can be optimized applying an iterative process.

### C. Linearly polarized lens performance

In this section the simulation results of a G-band LWA ( $f_0 = 160\text{GHz}$ ) illuminating a lens with a diameter  $D = 16\lambda_0$  and  $\epsilon_r = 2.32$ , are presented. The final geometrical values of this optimized double-slot iris are set to  $\alpha = 65.5$  deg,  $\rho = 0.48\lambda_0$  and  $w = 0.27\lambda_0$ . Fig. 2 shows the feed radiation pattern and

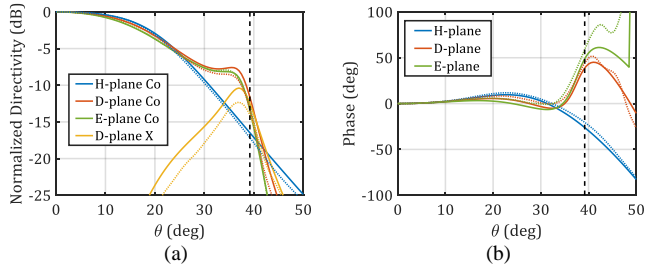


Fig. 2. (a) Feed radiation patterns and (b) phase at  $f_0=160\text{GHz}$ . Solid lines: SGF solution, dashed lines: full-wave simulations in CST.

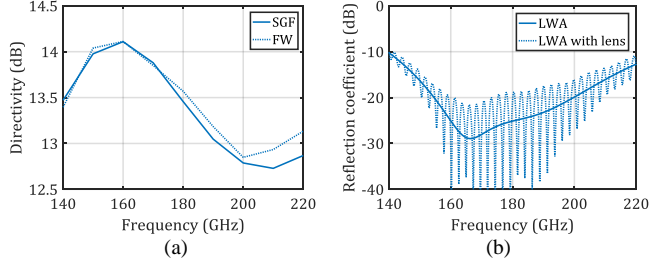


Fig. 3. (a) Feed maximum directivity over frequency (FW in CST) and (b) FW simulated reflection coefficient in EMPIRE-XPU.

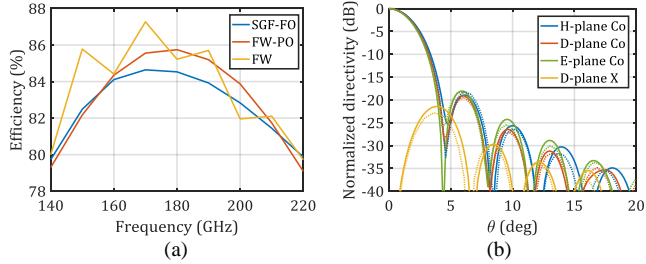


Fig. 4. (a) Lens aperture efficiency over frequency and (b) Simulated secondary radiation patterns at  $f_0$  (full: PO, dashed: FW with EMPIRE-XPU).

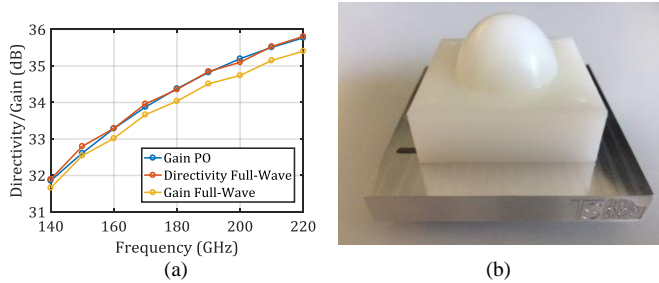


Fig. 5. (a) Directivity and gain as a function of the frequency (FW simulations with EMPIRE XPU) (b) Fabricated lens prototype.

phase at  $f_0$ , while Fig. 3a shows the maximum feed directivity over frequency. In both cases there is a good agreement between analytically computed results and full wave validation on CST. The maximum variation of the directivity over the entire frequency band is around 1 dB. Fig. 3b shows the comparison of the PO and full wave simulated reflection coefficient (including multiple reflections) in EMPIRE-XPU which is lower than  $-10\text{dB}$  over the whole operational bandwidth.

PO and full-wave simulations with EMPIRE-XPU have been performed for the lens together with the LWA, in order

to validate the optimization and with the aim of obtaining the lens far-field radiation patterns. Fig. 4a shows the comparison between aperture efficiencies calculated using these two methods and the FO approach. In Fig. 4b the secondary patterns are displayed at  $f_0$ . The good agreement between the PO and full-wave patterns proves that the multiple reflections and possible spillover do not have any significant impact on the lens antenna far fields, due to the lens low  $\epsilon_r$ . Fig. 5a shows the comparison between the gain calculated with the PO, and the full-wave directivity and gain simulated in EMPIRE-XPU. The maximum ohmic loss in the entire band is about  $0.5\text{dB}$  at  $220\text{GHz}$ . Fig. 5b shows the fabricated lens prototype.

### III. INTEGRATED DIELECTRIC GRATING POLARIZER

#### A. Concept and unit cell design

Dielectric grating polarizers are based on the transmission of orthogonal polarizations with  $90^\circ$  of phase shift. The gratings are present only in one axis, generating anisotropy in the structure effective  $\epsilon_r$ , which is higher for the polarization aligned with them. If a linear polarized field impinges the polarizer with a polarization rotated  $45^\circ$  with respect to the polarizer grid, the field can be decomposed in two orthogonal polarized waves in phase, parallel and perpendicular to the gratings (Fig. 6a). These components experiment different phase shifts when propagating along the polarizer, reaching  $90^\circ$  and so originating circular polarization in the transmitted wave.

As the polarizer will be integrated inside the lens, it seems convenient to use the same plastic material to fabricate both. In addition, low  $\epsilon_r$  materials improve significantly the reflection properties of the polarizer, enhancing in this way its efficiency and AR bandwidth. However, the  $\epsilon_r$  anisotropy is weaker for lower  $\epsilon_r$ , as the difference between the maximum and minimum possible effective  $\epsilon_r$  (around 2.5 and 1, respectively) is low. As a consequence, gratings with large height,  $h$  (Fig. 6c), are required to achieve the aimed  $90^\circ$  phase shift between the orthogonal components. On the other hand, the unit cell width or period,  $w$  (Fig. 6c), should stay small enough to avoid the appearance of grating lobes. These conditions result in a unit cell aspect ratio,  $h/w$ , higher than 7, which represents a big challenge in terms of cost-effective fabrication. Our strategy is to divide the unit cell height in four pieces (Fig. 6b), lowering in this way the  $h/w$  significantly, and fabricate them separately applying a milling technique. In addition, the gratings adopt pyramidal or roof geometry. This form not only provides the grid with mechanical stability, but also represents a smooth transition between air and the plastic material characteristic impedances. This fact enhances the polarizer reflection properties further, achieving in this way larger bandwidths. On top of that, the milling process is facilitated, as this geometry matches the also pyramidal milling tool cross section. A polarizer grating plate has already been fabricated with this technique in plastic material, with satisfactory results (Fig. 6c).

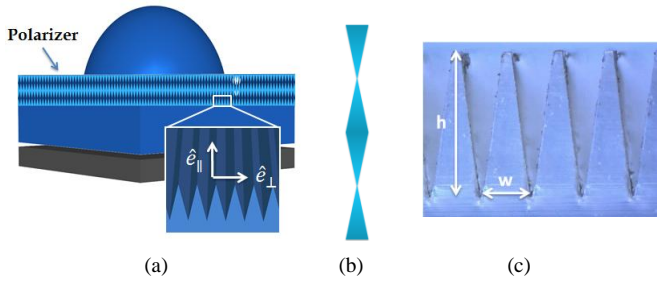


Fig. 6. (a) Simulation model of polarizer integrated in lens (b) Polarizer unit cell (front view) (c) Microscope picture of fabricated polarizer

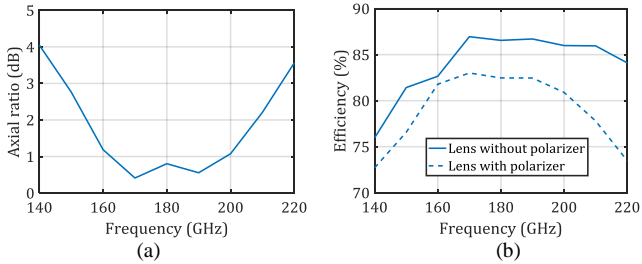


Fig. 7. Circularly polarized lens a) axial ratio b) aperture efficiency

### B. Circularly polarized lens

A first design for a polarizer integrated inside a lens with  $D = 16\lambda_0$  and  $\epsilon_r = 2.5$  has been carried out. The polarizer is optimized with means of FW simulations with EMPIRE XPU, following an iterative process. The first optimization is performed for broadside incidence with a single unit cell, using periodic boundary conditions. From this we extract the initial value for  $h$ . As a second step, the full polarizer is optimized embedded inside the lens (Fig. 6a), where the AR and aperture efficiency lens far-field are calculated for the full model. In this configuration, the LWA illuminates the polarizer with significant amplitude in  $\theta$  incident angles between broadside and  $40^\circ$  (Fig. 2a). The unit cell AR, optimized as a first step only for broadside incidence, experiments frequency shifts for obliquus incident angles. The lens far-field AR is the result of the integration of the polarizer AR for the full range of incident angles, weighted by the LWA illumination amplitude taper. By adjusting  $h$ , the lens AR is finally centred in the targeted frequency band, achieving a 3dB AR with 35% bandwidth (Fig. 7a). The FW simulated lens  $\eta_{ap}$  (including  $\eta_{tap}$  efficiency  $\eta_{so}$  and  $\eta_{ref}$ ) is higher than 75% for the whole frequency band (Fig. 7b).

## IV. CONCLUSION

In this work, broadband high-efficiency designs for linear and circularly polarized elliptical lenses fed by resonant leaky-wave antennas have been presented. The circular polarization is achieved by integrating a dielectric grating polarizer inside the lens, reaching in this way a very compact approach. A design with a lens and polarizer in plastic material has been reported, achieving an aperture efficiency higher than 80% over a 44% of relative bandwidth for the linear polarized lens, and an aperture efficiency higher than 75% with axial ratio

lower than 3dB over a relative bandwidth of 35% in case of the circularly polarized lens.

## ACKNOWLEDGMENT

This research is being co-financed by the European Union through the ERC Starting Grant LAA-THz-CC (639749) and IMST GmbH.

## REFERENCES

- [1] N. Llombart et al. "Fly's Eye Spherical Antenna System for Future Tbps Wireless Communications," 11th EuCAP, Paris, France, 2017.
- [2] D. Filipovic, S. Gearhart, and G. Rebeiz, "Double-slot antennas on extended hemispherical and elliptical silicon lens dielectric lenses," IEEE Trans. Microw. Theory Tech., vol. 41, no. 10, pp. 1738–1749, Oct. 1993.
- [3] X. Wu, G. V. Eleftheriades and T. E. van Deventer-Perkins, "Design and characterization of single- and multiple-beam mm-wave circularly polarized substrate lens antennas for wireless communications," IEEE Trans. Microw. Theory Tech, vol. 49, no. 3, pp. 431–441, Mar. 2001.
- [4] A. Neto, "UWB, Non Dispersive Radiation From the Planarly Fed Leaky Lens Antenna— Part 1: Theory and Design, " in IEEE Trans. Antennas Propag., vol. 58, no. 7, pp. 2238–2247, July 2010.
- [5] K. Konstantinidis, A. P. Feresidis, C. C. Constantinou, E. Hoare, M. Gashinova, M. J. Lancaster, and P. Gardner, "Low-THz Dielectric Lens Antenna With Integrated Waveguide Feed," IEEE Trans. On THz Science and Tech., vol. 7, no.5, pp. 572–581, Sept. 2017.
- [6] N. Llombart et al. "Novel Terahertz Antenna Based on a Silicon Lens Fed by a Leaky Wave Enhanced Waveguide," IEEE Trans. Antennas Propag., vol. 59, no. 6, pp. 2160–2168, June 2011.
- [7] M. Joyal and J. Laurin, "Analysis and design of thin circular polarizers based on meander lines," IEEE Trans. Antennas Propag., vol. 60, no. 6, pp. 3007–3011, June 2012.
- [8] D. Blanco et al. "Broadband and Broad-Angle Multilayer Polarizer based on Hybrid Optimization Algorithm for Low-cost Ka-band Applications," accepted in IEEE Trans. Antennas Propag.,
- [9] K.B.Cooper et al., "A Grating-Based Circular Polarization Duplexer for Submillimeter-Wave Transceivers," in IEEE Microwave and Wireless Components Letters, vol. 22, no. 3, pp. 108–110, Mar. 2012.
- [10] Y. Takashima et al., "Ultraviolet polarizer with a Ge subwavelength grating," in Applied Optics, vol. 56, no. 29, pp. 8224–8229, Oct. 2017.
- [11] T. Kämpfe et al., "Segmented subwavelength silicon gratings manufactured by high productivity microelectronic technologies for linear to radial/azimuthal polarization conversion," in Optical Engineering, vol. 53, Oct. 2014.
- [12] D. Blanco, E. Rajo-Iglesias, S. Maci and N. Llombart, "Directivity Enhancement and Spurious Radiation Suppression in Leaky-Wave Antennas Using Inductive Grid Metasurfaces," in IEEE Trans. Antennas Propag., vol. 63, no. 3, pp. 891–900, Mar. 2015.
- [13] M. Qiu, G. Eleftheriades, and M. Hickey, "A reduced surface-wave twin arc-slot antenna element on electrically thick substrates," in Proc. IEEE APS Int. Symp., Jul. 2001, vol. 3, pp. 268–271, vol. 3.
- [14] N. Llombart, A. Neto, G. Gerini, M. Bonnedal, and P. de Maagt, "Impact of mutual coupling in leaky wave enhanced imaging arrays," IEEE Trans. Antennas Propag., vol. 56, no. 4, pp. 1201–1206, Apr. 2008.
- [15] A. Neto, N. Llombart, G. Gerini, M. D. Bonnedal and P. de Maagt, "EBG Enhanced Feeds for the Improvement of the Aperture Efficiency of Reflector Antennas," in IEEE Trans. Antennas Propag., vol. 55, no. 8, pp. 2185–2193, Aug. 2007.
- [16] D. Blanco et al., "Low-Permittivity Elliptical Lens Fed by a Resonant Leaky-Wave Antenna for Wideband Wireless Communications," in EuCAP, London, United Kingdom, April 2018.
- [17] A. Neto, O. Yurduseven, N. Llombart, and A. Freni; "Antennas in reception," in EuCAP, Lisbon, Portugal, April 2015.
- [18] N. Llombart, B. Blazquez, A. Freni, and A. Neto, "Fourier Optics for the Analysis of Distributed Absorbers Under THz Focusing Systems," in Terahertz Science and Technology, IEEE TAP , vol. 5, no. 4, pp. 573–583, July 2015.